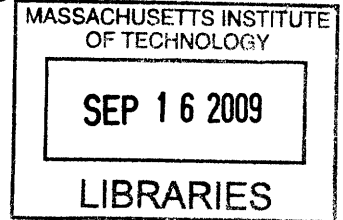


# Characterizing the Thermal Efficiency of Thermoelectric Modules

by

**Samuel S. Phillips**



Submitted to the Department of Mechanical Engineering in partial fulfillment of the requirements for the degree of

**Bachelor of Science**

at the

**Massachusetts institute of technology**

**June 2009**

**ARCHIVES**

© MIT. All Rights Reserved.

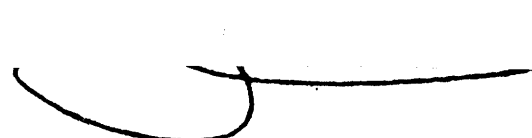
Signature of author.....

Department of Mechanical Engineering  
May 8, 2009

Certified by.....

Gang Chen  
Robson Professor of Mechanical Engineering  
Thesis Supervisor

Accepted by.....

  
John H. Lienhard  
Chairman, Undergraduate Thesis Committee



# Characterizing the Thermal Efficiency of Thermoelectric Modules

by

**Samuel S. Phillips**

**Submitted to the Department of Mechanical Engineering on May 8, 2009, in Partial Fulfillment of the Requirements for the Degree of Bachelor of Science in Mechanical Engineering**

## **ABSTRACT**

An experimental setup was designed and utilized to measure the thermoelectric properties as functions of temperature of a commercially available, bismuth telluride thermoelectric module. Thermoelectric modules are solid state semiconducting devices that act reversibly as both a heat pump and a power generator. The experimental setup encased the modules in an insulating container and thermal power was provided by a variable power cartridge heater, using type-K thermocouples to measure the temperature difference across the module. The measured parameters were compared against published data on a similar type of module. The thermal conductivity was measured within 21% of the accepted value on average, the Seebeck coefficient within 16%, the figure of merit within a factor two, and the thermal efficiency within 20% for low  $\Delta T$  of less than 25°C.

Thesis Supervisor: Gang Chen  
Title: Rohsenow Professor of Mechanical Engineering

## **ACKNOWLEDGEMENTS**

I would like to thank Prof Gang Chen for the opportunity to work on this project and for all the support and guidance throughout the semester. In addition, I would like to thank the other members of the NanoEngineering Group, particularly Andrew Muto and Daniel Kraemer, for their assistance and supervision on this project. Thanks goes to Hassan Mohamed for his help with calibration. Dr. Barbara Hughey also deserves mention for the lab equipment she lent me as does Prof. Richard Kimball for his enlightening discussions. Last, I would like to extend my thanks to my family and friends who have been there to help out and, every now and then, enjoy themselves along the way.

## TABLE OF CONTENTS

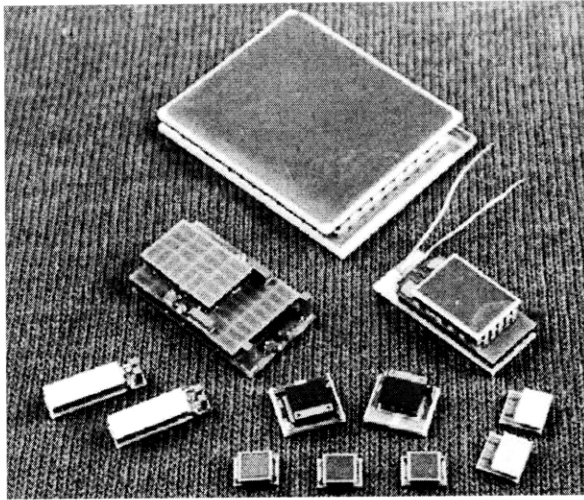
<b>ABSTRACT.....</b>	<b>3</b>
<b>ACKNOWLEDGEMENTS.....</b>	<b>4</b>
<b>TABLE OF CONTENTS.....</b>	<b>5</b>
<b>1. INTRODUCTION.....</b>	<b>6</b>
<b>2. BACKGROUND.....</b>	<b>7</b>
<b>3. MEASURING THERMOELECTRIC PARAMETERS.....</b>	<b>10</b>
<b>3.1 EXPERIMENTAL SETUP.....</b>	<b>10</b>
<b>3.2 CONFIRMING CONSTANT TEMPERATURE PROFILE .....</b>	<b>12</b>
<b>3.3 CALIBRATING HEAT LOSS .....</b>	<b>13</b>
<b>3.4 MEASURING THERMAL CONDUCTIVITY.....</b>	<b>13</b>
<b>3.5 MEASURING SEEBECK COEFFICIENT AND FIGURE OF MERIT.....</b>	<b>14</b>
<b>3.6 MEASURING CONVERSION EFFICIENCY.....</b>	<b>14</b>
<b>3.5.1 LOAD MATCHING.....</b>	<b>14</b>
<b>3.5.2 ELECTRICAL POWER OUTPUT.....</b>	<b>14</b>
<b>4. RESULTS.....</b>	<b>15</b>
<b>4.1 CONSTANT TEMPERATURE PROFILE.....</b>	<b>15</b>
<b>4.2 HEAT LOSS.....</b>	<b>15</b>
<b>4.3 THERMOELECTRIC PROPERTIES.....</b>	<b>16</b>
<b>4.3.1 THERMAL CONDUCTIVITY.....</b>	<b>16</b>
<b>4.3.2 SEEBECK COEFFICIENT.....</b>	<b>17</b>
<b>4.3.3 FIGURE OF MERIT.....</b>	<b>18</b>
<b>4.3.4 THERMAL EFFICIENCY.....</b>	<b>19</b>
<b>5. DISCUSSION.....</b>	<b>19</b>
<b>6. CONCLUSIONS.....</b>	<b>21</b>
<b>WORKS CITED.....</b>	<b>23</b>

## 1. INTRODUCTION

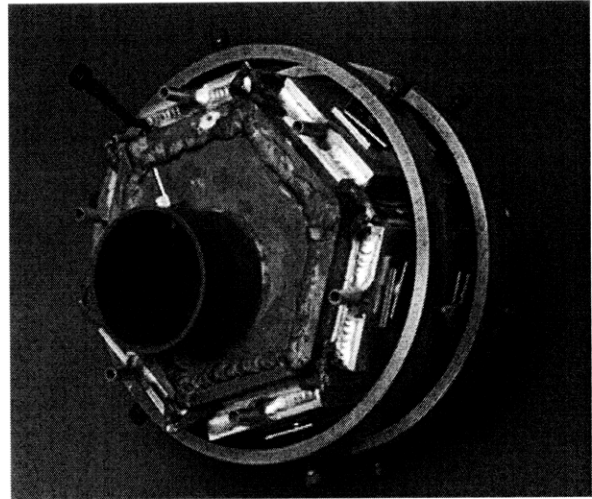
The problem presented in this paper is that of characterizing the first law efficiency of a thermoelectric module via a novel experimental technique. Thermoelectric modules are solid state devices based on the principle of the Seebeck-Peltier effect that convert thermal energy to electrical energy and vice versa. Apply a temperature difference to the module, and a voltage appears across the terminals. Alternatively, and more importantly, reversibly, applying a voltage to the terminals of the module produces a temperature difference across its faces. This duality allows thermoelectric modules to act both as a power generator, given a heat source, and a heater or refrigerator when supplied with electrical power. Figure 1a shows thermoelectric modules similar to the one used for this paper<sup>1</sup>.

Thermoelectric modules are used across a variety of industries for both power generation and heating / cooling applications. For instance, they are used as small scale, precision temperature control devices for electronics. Thermoelectric devices are also playing a significant role in the renewable energy movement, used in such applications as solar thermal generators. Generally, they are used wherever there is a small temperature gradient that can be exploited for power generation. For example, auto manufacturer BMW is currently developing a type of thermoelectric module that will extract electrical energy from the waste thermal energy left in the exhaust stream<sup>2</sup>.

This paper discusses a method for determining how efficiently a thermoelectric module operates as a power generator as well as measuring other system parameters. An external cartridge heater heats the thermoelectric module from one side while the other is thermally coupled to a heat sink, providing a measurable temperature difference across the faces of the device. The electrical leads can be then be configured to provide power to an external load. Comparing the thermal power supplied to the thermoelectric module to the power dissipated across the load determines the overall first law efficiency of thermoelectric conversion.



(a)



(b)

**Figure 1: (a) A variety of thermoelectric modules similar to the one discussed in this paper. (b) Thermoelectric modules attached to the exhaust of a BMW prototype. This device won an OkoGlobe Award in 2008. (Fig. 1a courtesy of Marlow Industries, Inc. Fig. 1b courtesy of [www.motorauthority.com](http://www.motorauthority.com))**

## 2. BACKGROUND

Thermoelectric devices are based on a principle known as the Seebeck-Peltier effect, which describes the reversible conversion of thermal energy to electrical energy. Figure 2 shows a schematic of the Seebeck-Peltier effect as seen in a thermoelectric module. If a current is supplied through the material, this will produce a temperature difference across the faces. If a heat source is applied, then a voltage drop will appear across the electrical terminals of the device. This is due to a movement of charge carriers, either electrons or holes depending on the material, from one face to the other due to a change in the electrical potential inside the material. The charge carriers for n-doped semiconductors are electrons and are positively charged holes for p-doped semiconducting materials. As one face heats, the kinetic energy of the mobile charge carriers on the hot side increases and they gradually start to diffuse across the energy gradient to the cold face. Charge carriers continue moving across the gradient until a sufficient amount of charge has accumulated on the cold face and so the difference in charge produces an electric potential that exactly counteracts that produced by the Seebeck-Peltier effect. For charges to continue to flow either the temperature difference / current must be increased or the material must be connected to a closed circuit.

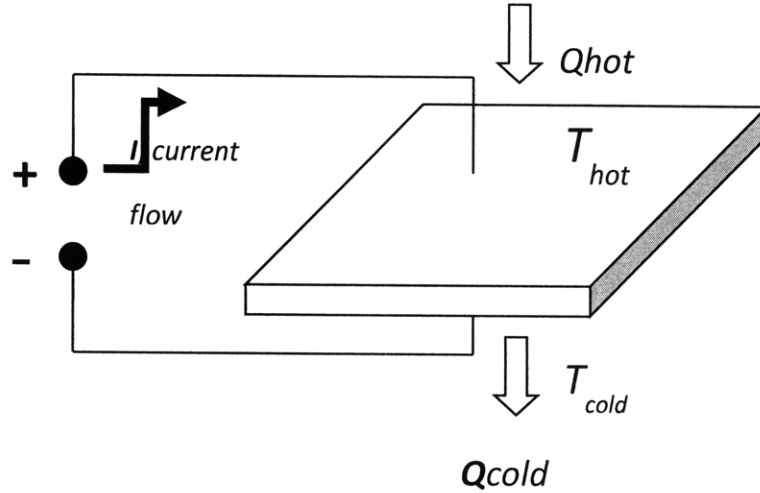


Figure 2: Energy flow diagram for the Seebeck-Peltier effect.

The voltage produced when a temperature difference is present across the device is called the Seebeck voltage. For a material with a temperature difference  $\Delta T$  and an induced voltage  $V$ , the Seebeck coefficient is defined as follows<sup>3</sup>:

$$S = -\frac{V}{\Delta T} \quad (1)$$

However, for even the best thermoelectric materials, the Seebeck coefficient is on the order of microvolts per degree Kelvin temperature difference. To increase this voltage to useful levels, a large number (~100 or more, usually) of individual thermoelectric elements are connected

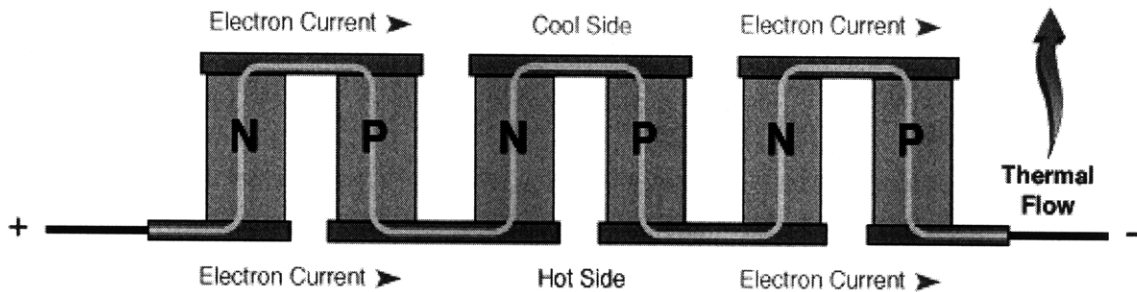


Figure 3: Thermoelectric elements in a module alternate between N and P doped materials in order to create a continuous electrical path for elements thermally loaded in parallel.



electrically in series but thermally in parallel. Figure 3 shows how alternating between n and p doped materials allow for a continuous electrical path while maintaining parallel thermal loading<sup>4</sup>. Usually sandwiched between slabs of a material with a high thermal conductivity but low electrical conductivity, these components form a thermoelectric module when assembled.

The first law efficiency,  $\eta$ , of a thermal electric module is the ratio of the electrical power delivered,  $Q_{elec}$ , and the thermal power input to the hot side of the device,  $Q_{hot}$ :

$$\eta = \frac{Q_{elec}}{Q_{hot}} \quad (2)$$

The heat transfer through the module is given by Fourier's law of conduction:

$$\dot{Q}_{hot} = \frac{KA}{t} \Delta T \quad (3)$$

where  $K$  is the thermal conductivity,  $A$  is the surface area, and  $t$  is the module thickness.

The electric power is determined the resistive heating relation:

$$\dot{Q}_{elec} = \frac{V^2}{R} \quad (4)$$

where  $R$  is the total electrical resistivity, including the load resistance and the internal resistance from the module. The resistivity can be measured directly while the thermal conductivity must be measured implicitly by determining the heat transfer through the module when it is not loaded.

To achieve maximum efficiency, the thermoelectric material must minimize the heat throughput while maximizing the current because the heat transferred from the cold side to the heat sink is wasted energy that is not converted. This amounts to maximizing the electrical conductivity of the material while minimizing the thermal conductivity. The thermoelectric figure of merit,  $Z$ , is a measure of a material's relative effectiveness of transporting electrical compared to thermal energy:

$$Z = \frac{S^2 \cdot T_{ave}}{RK} \quad (5)$$

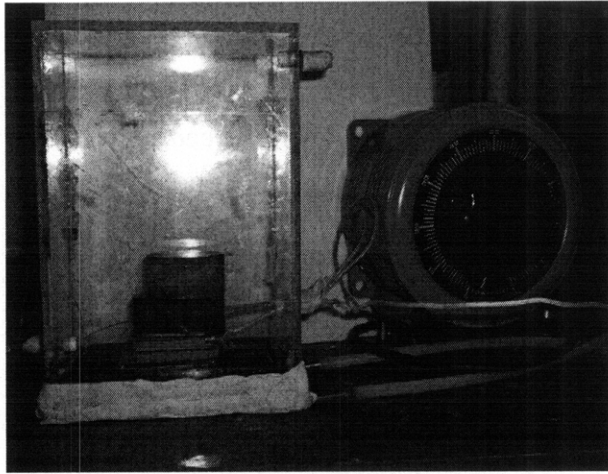
where  $T_{ave} = (T_{hot} + T_{cold})/2$  is the temperature averaged across the thickness of the module.

### 3. MEASURING THERMOELECTRIC PARAMETERS

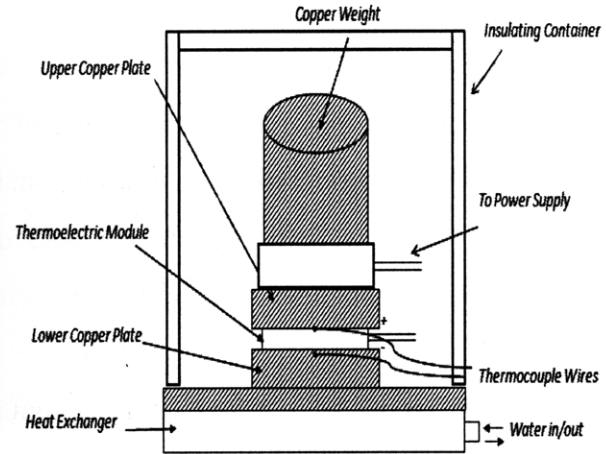
A novel experimental setup was developed to characterize the thermal properties of a thermal electric module. Significant effort went into creating a repeatable setup that would accurately simulate the assumptions made in the theoretical model so as to reliably compare the measured results with the manufacturer's given performance specifications. Specifically, care was taken to ensure minimal heat loss to the environment and to be able to obtain an accurate estimate of it and to create a constant temperature across the surface of the module. Each of these assumptions was verified experimentally.

#### 3.1. Experimental Setup

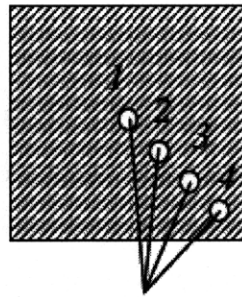
The final iteration of the experimental setup is seen in Figure 4. The setup consists of a thermoelectric module sandwiched between two copper plates. One type K thermocouple is embedded into the top copper plate and four in the bottom plate to measure the temperature difference across the faces of module. See Figure 4c for the arrangement of the thermocouples. The four thermocouples on the bottom plate are dispersed at select distances from the center of the plate. This is used to validate the assumption of a constant temperature across the face of the device. In addition, since the thermal conductivity of copper is approximately two orders of magnitude higher than that of the thermoelectric module, the presence of the copper blocks is assumed to be negligible because much larger thermal gradients would most likely manifest themselves in the module. The thermocouples were calibrated against one another by noting their readings when at ambient temperature and subtracting the difference.



(a)



(b)



*Holes for thermocouples*

(c)

**Figure 4: (a) Photo and (b) labeled diagram of the experimental setup. (c) shows the placement of the thermocouples on the cold face of the module.**

Thermal energy is provided by a cartridge heater capable of producing 400W maximum. The cartridge heater, essentially a precision, temperature-constant resistive element, is installed inside a mild steel sheath to allow for more even temperature distribution and is powered by an external transistor hooked up to a standard 120V wall outlet. With this power supply configuration, the thermal power output of the cartridge heater could be varied continuously from 0 to 400W. The cartridge heater power was calculated by measuring the voltage across the transformer and using the resistive power generation formula (Eq. 4). A cold water heat exchanger was used as the heat sink for the cold side of the module.

Surrounding the entire setup was an insulating Plexiglas box that also helped to create a repeatable environment for the measurements. By isolating the rest of the setup instead of in the ambient air, the heat loss mechanism switched from natural convection to forced convection. This allowed for a better estimate of the thermal losses from the setup. The power supply and thermocouple wires were run through a hole in the insulating container. The holes and the intersection of the container and the heat exchanger were sealed with plasticine to prevent air leakage.

Measurements were taken using a digital multimeter and a thermocouple reader. The input power to the cartridge heater from the transformer was adjusted in increments of 5V and the device was allowed to reach thermal equilibrium before taking any measurements. The thermocouples were connected to the thermocouple reader to measure the temperature difference. For measuring the power input and the Seebeck coefficient, the electrodes from the multimeter were placed across the terminals such that the positive electrode was on the hot face of the module. To measure the power dissipated by the module resistance, a potentiometer was attached to the electrical terminals and was set to the appropriate resistance. The electrodes from the multimeter were connected to the potentiometer and the voltage drop across the resistor was found for select temperatures, relating the voltage to the power dissipated using Equation 4.

The thermoelectric module used in this experiment was a bismuth telluride module, model name DT12, manufactured by Marlow Industries, Inc.

### **3.2 Confirming Constant Temperature Profile**

In the theoretical analysis of the thermoelectric module's properties, the temperature is assumed to be constant over the entire surface of the device. To test this assumption, four type-k thermocouples were inserted into the lower copper plate at varying distances from the center of the plate, as seen in Figure 4c. With a thermoelectric module in place, the temperature of the lower plate in all four locations was measured for selected power outputs of the cartridge heater and then plotted to compare the temperature profile across the face of the device for  $I_{heater}$  from 0 to 3.3 Amps. Using similar logic as before, the temperature gradients in the copper can be assumed to correspond to those in the module because of the large difference in thermal

conductivities. In the ideal case, all thermocouple locations would measure the same temperature.

### 3.3 Calibrating Heat Loss

Obtaining an accurate estimate of the heat loss in the experimental is necessary to calculate the thermal conductivity of a thermoelectric module. Using the principal of conservation of energy and assuming that, at equilibrium, the thermal energy from the cartridge heater either transfers through the module or is dissipated, the heat loss is found to be the difference between the power provided by the heater and the energy transferred through the thermoelectric module, or  $Q_{loss} = Q_{heater} - Q_{module}$ . The heat input,  $Q_{heater}$  is determined by the voltage across the transformer.  $Q_{module}$  is determined using Fourier's law of conduction (Eq. 3).

However, the thermal conductivity of the module is unknown. Substituting a material of known thermal conductivity with similar dimensions as the module allows the heat losses to be estimated. A 2.25 square inch (14.5 cm<sup>2</sup>), .25 inch (0.6 cm) piece of Plexiglas with thermal conductivity  $K = 0.18^5$  W/mK was inserted in lieu of the module. The input power was varied and heat loss was calculated over a hot side temperature range of 30°C and 120°C.

### 3.4 Measuring Thermal Conductivity

The thermal conductivity of a thermoelectric module is needed for comparing the module's relative rate of thermal to electrical transfer. To measure this parameter, thermoelectric module's electrical leads were shorted in order to isolate the module's thermal properties. The temperature difference across the faces was measured for the temperature range of  $T_{hot}$  from 25°C to 150°C. The heat transfer through the module can be calculated from the difference of the supplied power from the heater and the estimated heat loss at that temperature. By rearranging Eq. 3 and solving for  $K$ , the thermal conductivity of the module can be calculated from the temperature difference, the calculated heat transfer through the device, and its geometric properties.

### **3.5 Measuring Seebeck Coefficient and Figure of Merit**

To obtain values for the Seebeck coefficient of the module, the voltage drop across the electrical leads of the module and the temperature difference between the faces were found for a range of hot side temperatures. The measured data can be related to the Seebeck coefficient via Equation 1. However, this is the Seebeck coefficient for the entire module. To find  $S$  for each individual leg of the module, the result from Equation 1 was divided by the total number of legs, which were counted manually. The figure of merit,  $ZT$ , was directly calculated from the measured values of  $S$ ,  $K$ , and  $R$  by the relationship given in Equation 5.

### **3.6 Measuring Conversion Efficiency**

#### **3.6.1 Load Matching**

The maximum efficiency of a thermoelectric module occurs when the current output of the module is maximized as well. The current is maximized when the resistive load on the module is equal to the internal resistance of the module itself<sup>6</sup>. A variable potentiometer was electrically connected across the terminals of a module at thermal equilibrium at 41°C and the current was monitored as the resistance was changed. The maximum current was found to occur at a resistance of about 2 Ohms. This resistance was then used for all subsequent measurements.

#### **3.6.2 Electrical Power Output**

Setting the potentiometer to 2 Ohms, the temperature of the hot side was varied from 25°C to 150°C and the heat transfer rate through the module was calculated. For each temperature, the current across the terminals was measured and the electrical power was calculated via Equation 4. Using Equation 2 by taking the ratio of the electrical power output to the thermal power supplied to the module, the first law efficiency of the thermoelectric module can be determined.

## 4. RESULTS

### 4.1 Temperature Profile

The temperature distribution across the cold face of the thermoelectric module for each of the four embedded thermocouples is plotted in Figure 5 as a function of input current. Figure 5 shows that the temperature distribution across the plate as measured at each location is nearly uniform until  $T_{\text{cold}} \sim 40^{\circ}\text{C}$  where the curves begin to diverge from one another. Nevertheless, the maximum deviation is 9% meaning that the constant temperature profile assumption is valid to within 9%, with much greater accuracy at  $T_{\text{cold}} < 40^{\circ}\text{C}$ . Thus, the temperature can be measured from

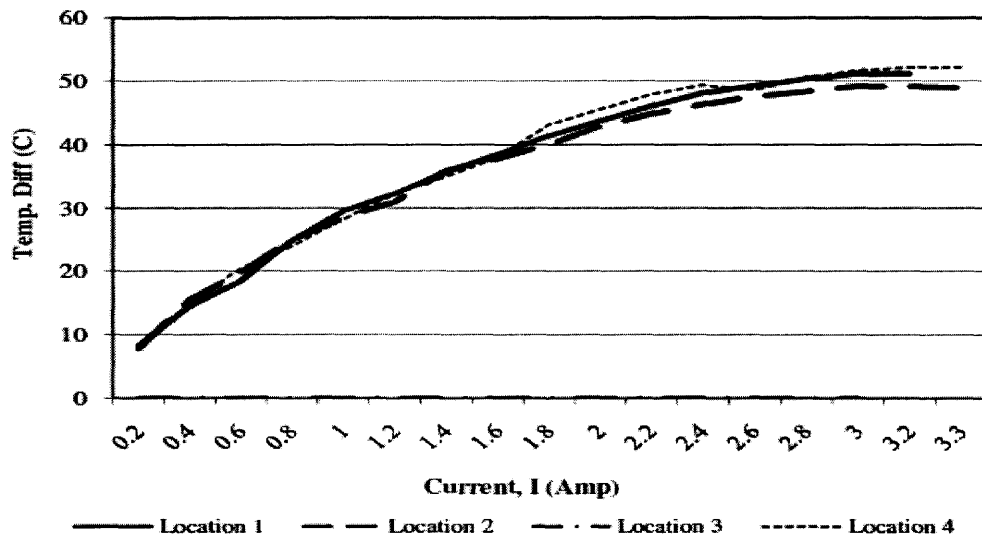


Figure 5: Temperature measurements for each thermocouple location, confirming the constant temperature profile assumption. (Courtesy of Hassan Mohamed)

any of the four thermocouple locations without significantly affecting the results. It should be noted that the majority of data collected fell below this value, with only 20% of data points above  $40^{\circ}\text{C}$ .

### 4.2 Heat Loss

The heat loss,  $Q_{\text{loss}}$ , as function of the hot side temperature,  $T_{\text{hot}}$ , is shown in Figure 6 for  $T_{\text{hot}}$  ranging from  $20^{\circ}\text{C}$  to  $120^{\circ}\text{C}$ . The heat loss was found to be a linear function of  $T_{\text{hot}}$  with a linear fit of  $Q_{\text{loss}} = 0.18T_{\text{hot}} - 4.1$ . In further calculations, this linear fit was used to interpolate

between measured data points to estimate heat losses. The model had a coefficient of determination, or  $R^2$  value, of 0.993 yielding an accuracy of  $\pm 2\%$  from measured values.

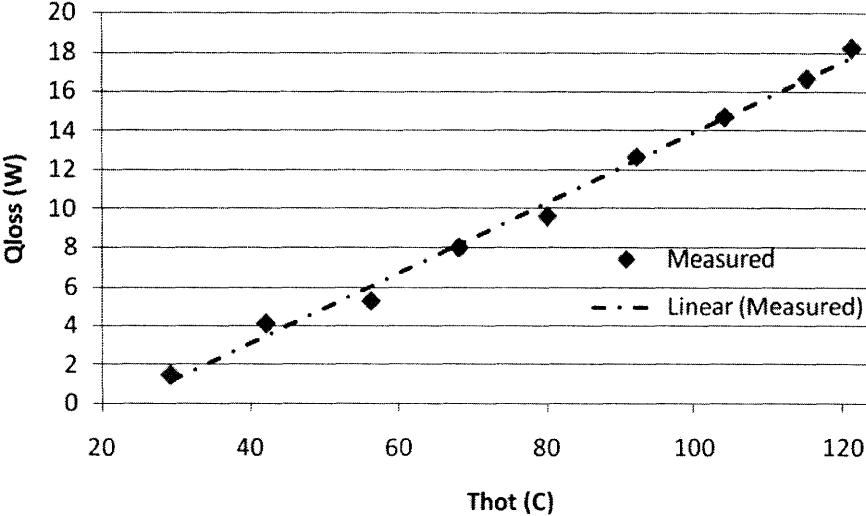


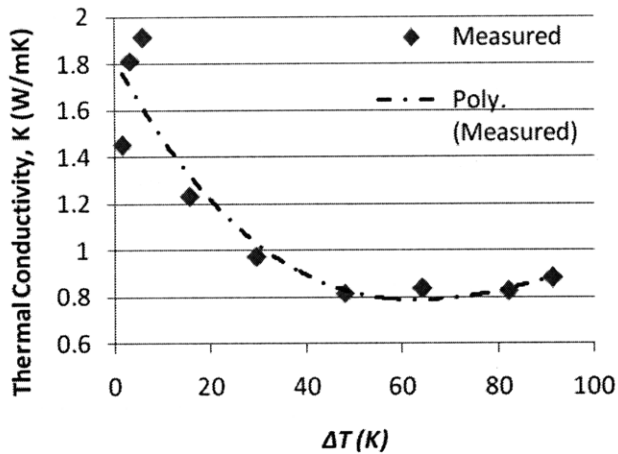
Figure 6: Heat loss ( $Q_{loss}$ ) vs. hot side temperature ( $T_{hot}$ ), both measured data and linear fit.  $R^2 = 0.993$  for an error of  $\pm 2\%$

### 4.3 Thermoelectric Properties

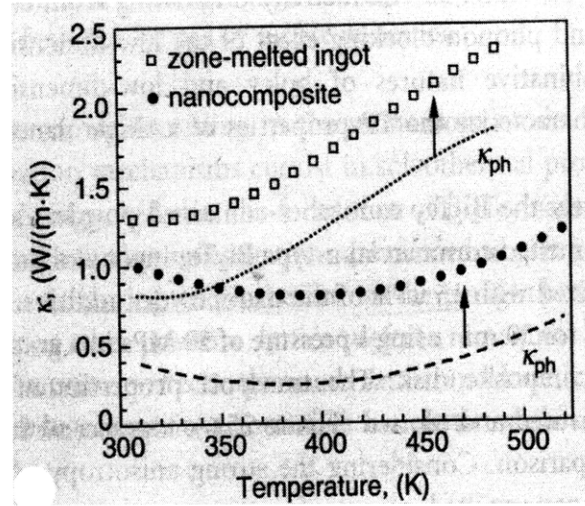
#### 4.3.1 Thermal Conductivity

The experimental setup yielded measurements of the thermoelectric module’s thermal and electrical properties, each with varying degrees of agreement with the accepted values. The thermal conductivity, shown below in Figure 7a, was measured to within 21% of the accepted, published data seen in Figure 7b.





(a)



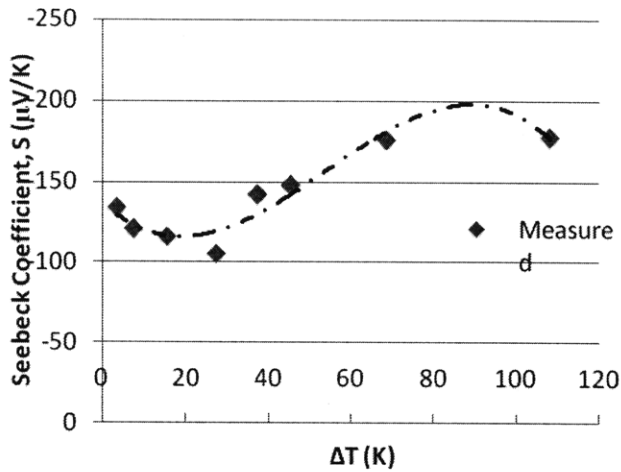
(b)

**Figure 7: (a) Measured thermal conductivity vs.  $\Delta T$  for DT12 model with a polynomial fit to show data trends. (b) published data for a comparable bismuth telluride module<sup>3</sup>. Temperature shown is  $T_{\text{hot}}$  with  $T_{\text{cold}}$  maintained at 300K.**

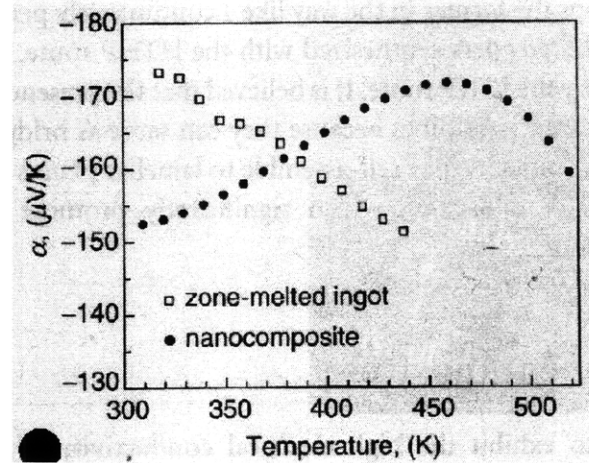
The data shows a decreasing trend as  $\Delta T$  increases. At first thought, this trend seems counterintuitive as temperature increases, the average vibrational energy of the crystal lattice increases as does the kinetic energy of the charge carriers because of the induced electrical potential. Higher phonon energy means higher frequency of vibration giving a higher rate of interaction and phonon transfer between adjacent molecules. However, this is apparently not the case for the thermoelectric module at hand. The decrease in thermal conductivity must be linked to other factors involved in the energy transfer.

#### 4.3.2 Seebeck Coefficient

Measured results for the Seebeck coefficient as a function of temperature difference of are shown in Figure 8a alongside published data for a comparable bismuth telluride thermoelectric module (Figure 8b). Note here that the published data uses the variable  $\alpha$  instead of  $S$  to represent the Seebeck coefficient.



(a)

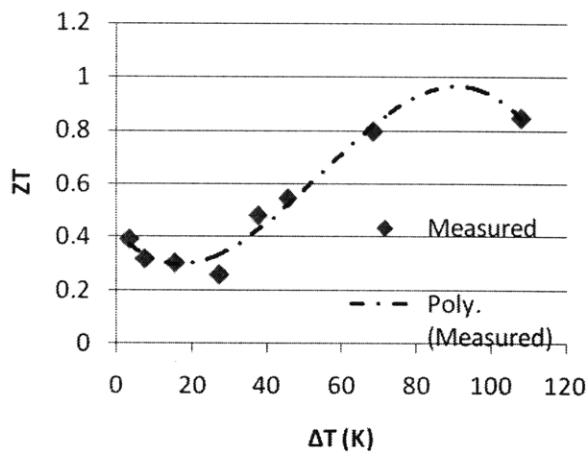


(b)

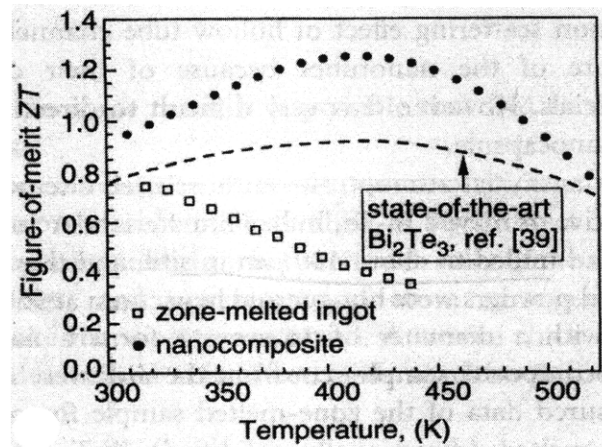
Figure 8: (a) Seebeck coefficient vs. temperature difference for DT12 module with a polynomial fit to show data trends. (b) published data for a comparable bismuth telluride module<sup>3</sup>.

#### 4.3.3 Figure of Merit, ZT

The figure of merit, ZT, was calculated via Equation 5 using measured results for the Seebeck coefficient and thermal conductivity over a temperature range of 120°C. Figure 9 plots both the measured data for the DT12 module (Figure 9a) and the published values for a similar module (Figure 9b).



(a)



(b)

Figure 9: Comparison of measured ZT vs.  $\Delta T$  for DT12 module (a) to published data for a comparable bismuth telluride module<sup>3</sup>.

### 4.3.4 Thermal Conversion Efficiency

The first law efficiency of the DT12, a gauge of its effectiveness at converting thermal energy to electrical energy, was calculated as function of  $\Delta T$  using Equation 2 with measured values for the electrical and thermal power. The result is plotted in Figure 10a with 10b a graph of theoretical thermoelectric efficiencies for select values of  $ZT$  for comparison<sup>7</sup>.

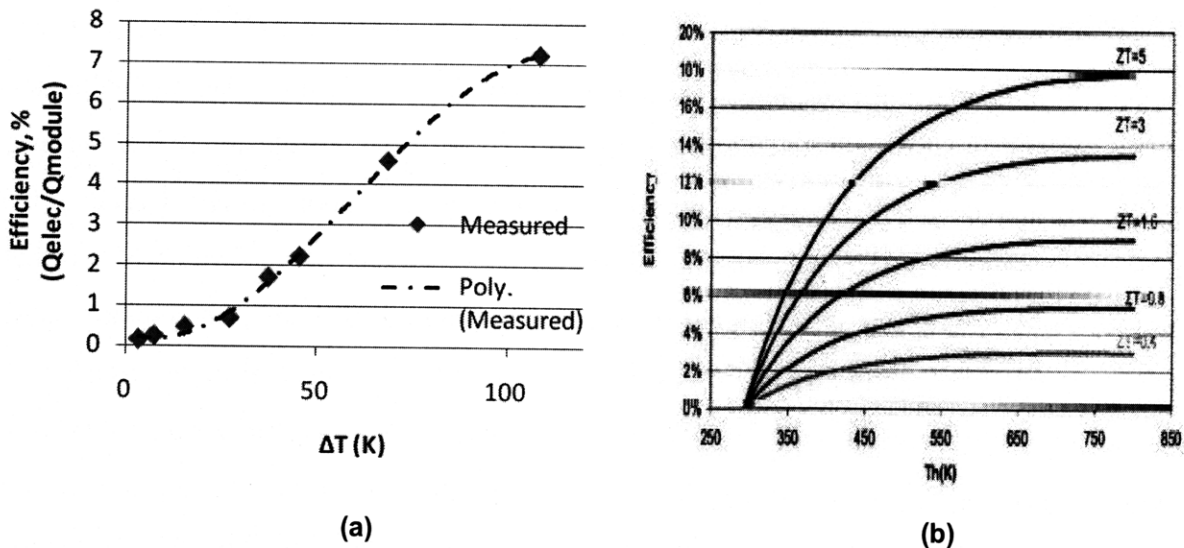


Figure 10: Comparison of efficiency vs. temperature for measured data (a) and published data for select values of  $ZT$  (b). Again, the temperature presented is  $T_{hot}$  and  $T_{cold}$  is held at 300K.

## 5. DISCUSSION

Overall, the measured data is in reasonable agreement with the general trends seen in the published data for the data set labeled “nanocomposite”, which is in fact a mixture of commercially available thermoelectric materials and bismuth telluride nanoparticles. This can be noted by comparing the functional responses of the measured and published data: they rise and fall together and appear to be governed by the same family of functions (linear, exponential, etc.) However, the accuracy of the measurements varies widely from one parameter to the next and changes as  $\Delta T$  changes. The percent error in the thermal conductivity,  $K$ , varies from nearly 75% at  $\Delta T = 5^\circ\text{C}$  to 5% at  $\Delta T = 100^\circ\text{C}$ , with the results matching more closely as  $\Delta T$  increases. The error seen in the Seebeck coefficient ranges from 22% at  $\Delta T = 25^\circ\text{C}$  to 13% at  $\Delta T = 110^\circ\text{C}$ . For

the figure of merit,  $ZT$ , the correspondence between the data sets is relatively constant over the temperature range, although the values disagree by a factor of about one and a half. Finally, the thermal efficiency of the module,  $\eta$ , is seen to increase logarithmically with  $\Delta T$  and has relatively good correspondence at low  $\Delta T$  with the theoretical data presented in Figure 10b. Using an average value of  $ZT$  of 0.4, the percent difference in measured efficiency ranges from 12% at  $\Delta T = 20^\circ\text{C}$  to being off by a factor of 7 at  $\Delta T = 110^\circ\text{C}$ .

Comparing the graphs of efficiency and figure of merit lead to an interesting conclusion. Although the average of the calculated  $ZT$  values is 0.48, the efficiency graph corresponds far better with the curves for higher  $ZT$  values, with  $ZT = 1.6$  providing the best match. However, this leads to a conclusion that there was some compounded error in the experimental setup that led to discrepancies in both efficiency and figure of merit. This conclusion arises because the average calculated  $ZT$  is 0.48, which falls slightly below the commonly accepted value of 0.5 for the cutoff as being considered a thermoelectric device. However, the  $ZT$  value of 1.6 that the efficiency curves suggests is far higher than the  $ZT$  of top of the line, commercially available modules which is currently around 1.2, as seen in Figure 9b.  $ZT$  values of up to three have been approached in research laboratories using novel, nanotechnology-based materials to increase the electrical conductivity of the material while creating random particulate grains that scatter phonons, thereby decreasing the thermal conductivity. The Marlow DT12 is just a commercially available bulk module so  $ZT$  values of 1.6 are not possible.

Another trend seen in the data leads logically to one the first plausible sources of error. The data for the thermal conductivity, figure of merit and Seebeck coefficient all show significant improvements in reduction of error from the published values as  $\Delta T$  increases. Even though the error grows with temperature for thermal efficiency, it can be shown that the shape of the curves become more alike as  $\Delta T$  becomes larger. This can be linked to inherent inaccuracies in the temperature measurement caused by the relative accuracy of the type-K thermocouples embedded in the copper plates. Type-K thermocouples have an average accuracy of only  $\pm 1.5^\circ\text{C}$  so at low temperature differences, this inaccuracy can account for a large percentage of the actual value. At  $\Delta T = 10^\circ\text{C}$ , the error in the measurement is up to 30%, or  $3^\circ\text{C}$ . However, as the temperature difference increases, this effect becomes less and less significant, with an error of only 3% at  $\Delta T = 100^\circ\text{C}$ .

Other possible sources of error include the electrodes of the thermocouple reader which used non-matching metals, leading to external voltage sources that can either add or detract from the potential produced by the module. Also, in calculating the figure of merit, module parameters were assumed constant with temperature although they should be assumed to change. Making the constant parameter assumption leads to an error of not more than 10%<sup>3</sup>.

## 6. CONCLUSIONS

An experimental setup was designed and utilized to measure the thermoelectric properties as functions of temperature of a commercially available, bismuth telluride thermoelectric module. Thermoelectric modules are solid state semiconducting devices that act reversibly as both a heat pump and a power generator. The experimental setup encased the modules in an insulating container and thermal power was provided by a variable power cartridge heater, using type-K thermocouples to measure the temperature difference across the module.

The measured parameters were compared against published data on a similar type of module. The thermal conductivity was measured within 21% of the accepted value on average, the Seebeck coefficient within 16%, the figure of merit within a factor 1.5, and the thermal efficiency within 20% for low  $\Delta T$ . To further improve these measurements, higher resolution temperature measurement devices such as thermistors should be used. Also, more careful attention should be paid to maintaining consistent materials throughout and to use temperature dependent parameters in calculations.

## WORKS CITED

- [1] “DT Series Thermoelectric Modules”. [www.marlow.com](http://www.marlow.com). August 2007.
- [2] Hall, Kenneth. “Early look at BMW’s next wave of Efficient Dynamics Technology”. 9 March 2009. [www.motorauthority.com](http://www.motorauthority.com)
- [3] Rowe, D.M., ed. *Thermoelectrics Handbook*. Boca Raton, FL. Taylor and Francis Group, LLC. 2006.
- [4] “Thermoelectric Power Generation – 12 Most Frequently Ask Questions”. [www.tellurex.com](http://www.tellurex.com). May 2008.
- [5] “Typical Thermal Properties”. [www.plexiglass.com](http://www.plexiglass.com). February 2006.  
< <http://www.plexiglas.com/tds/4b.pdf> >
- [6] Muto, Andrew. “Device testing and characterization of thermoelectric nanocomposites”, Dept. of Mechanical Engineering, MIT, 2008.
- [7] Bertreau, Phillipe. “Novel thermoelectric materials development, existing and potential applications, and commercialization routes”. Dept. of Materials Science and Engineering, MIT. 2006.